AJNR

Diffusion-weighted MR Imaging After Angioplasty or Angioplasty Plus Stenting of Arteries Supplying the Brain

Horst J. Jaeger, Klaus D. Mathias, Robert Drescher, Elke Hauth, Georg Bockisch, Eren Demirel and Hans Martin Gissler

AJNR Am J Neuroradiol 2001, 22 (7) 1251-1259
http://www.ajnr.org/content/22/7/1251

AJNR Am J Neuroradiol 22:1251–1259, August 2001

Diffusion-weighted MR Imaging After Angioplasty or Angioplasty Plus Stenting of Arteries Supplying the Brain

Horst J. Jaeger, Klaus D. Mathias, Robert Drescher, Elke Hauth, Georg Bockisch, Eren Demirel, and Hans Martin Gissler

BACKGROUND AND PURPOSE: **There has been concern regarding the safety of revascularization procedures of vessels supplying the brain vessels because of the risk of cerebral embolization during the procedure. We have observed a high incidence of hyperintense lesions on diffusion-weighted MR images of the brain after stenting at the carotid bifurcation. The hypothesis of this study is that diffusion-weighted MR imaging of the brain can reveal new diffusion abnormalities after angioplasty or angioplasty plus stenting of arteries supplying the brain, other than at the carotid bifurcation. Therefore, we prospectively obtained diffusion-weighted MR images of the brain before and after such revascularization procedures.**

METHODS: **Thirty-seven revascularization procedures were performed in 32 patients. Eleven interventions were performed at the distal internal carotid artery, two at the external carotid artery, two at the common carotid artery, five at the innominate artery, five at the vertebral artery, and 12 at the proximal subclavian artery. Diffusion-weighted MR imaging of the brain was performed before and 24 hours after the procedures.**

RESULTS: **After eight (22%) of 37 procedures, new hyperintensities were visible on the diffusion-weighted MR images. With six of these eight procedures, the hyperintensities occurred in the vascular territory supplied by the treated vessel. In total, 35 new cerebral lesions could be seen, 33 (94%) of which occurred in the vascular territory supplied by the treated vessel. None of the patients in whom new diffusion abnormalities were found had new neurologic symptoms or deficits. No new lesions could be seen after procedures at the subclavian artery.**

CONCLUSION: **Revascularization procedures of arteries supplying the brain were associated with new lesions on the diffusion-weighted MR images of the brain after 22% of the procedures, provided that MR imaging could be performed, indicating the occurrence of cerebral microemboli during such procedures. Diffusion-weighted MR imaging of the brain can be used as a tool to assess the impact of modifications of procedural technique and/or the use of cerebral protection devices on the occurrence of such lesions.**

During the last years, interventional revascularization procedures of vessels supplying the brain have been developed as an alternative to medical and/or surgical treatment (1–13). However, there has been concern regarding the safety of such interventions because of the risk of cerebral embolization during the procedure (14–16).

For stenting of the carotid bifurcation, it has been assumed that the cause of the majority of the complications is distal embolization of plaque material during the procedure (1–4). The incidence of asymptomatic emboli detected by transcranial Doppler monitoring for balloon angioplasty and stent implantation at the carotid bifurcation exceeded 90% (16).

At present, diffusion-weighted MR imaging is the most sensitive tool to detect early cerebral ischemia (17–23). It has been used to detect structural damage of the brain due to silent embolism during cerebral angiography and stenting at the carotid bifurcation (24–26). We have seen new postprocedural lesions detected by diffusion-weighted MR imaging after 29% of stenting procedures at the carotid bifurcation for high-grade stenosis in cases in which MR imaging could be performed (H.J. Jaeger, unpublished data, 2001).

The hypothesis of this study is that diffusion-weighted MR imaging of the brain can reveal new

Received September 27, 2000; accepted after revision January 16, 2001.

From the Department of Radiology, Staedtische Kliniken Dortmund, and the Department of Radiology und Mikro-Therapie, University Witten/Herdecke, Dortmund, Germany.

Address reprint requests to Horst J. Jaeger, MD, Beurhausstrasse 40, D-44139 Dortmund, Germany.

TABLE 1: Characteristics of lesions and interventions

Treated Vessel	Site of Lesion	Etiology	Type of Intervention (Diameter in mm)
11 × ICA	5 × cavernous	5 × AS	2 × PTA (2.5 mm; 3.5 mm)
			3 × attempts to treat
	2 × petrosal	2 × AS	2 × PTA (2.5 mm; 3.5 mm)
	4 × cervical	3 × FMD	4 × PTA (3–5 mm)
		1 × RES	
2 × ECA	2 × origin	2 × AS	2 × PTA (4 mm; 5 mm)
2 × CCA	2 × origin	2 × AS	2 × balloon-expandable stent (8 mm; 9 mm)
5 × IA	5 × origin	5 × AS	3 × balloon-expandable stent (8 mm)
			1 × self-expandable stent (10 mm)
			1 × PTA (10 mm)
5 × VA	1 × V4	1 × AS	1 × balloon-expandable stent (3.5 mm)
	1 × V2	1 × AS	1 × PTA (3.5 mm)
	3 × V1	3 × AS	2 × balloon-expandable stent (3.5 mm; 4.5 mm)
			1 × PTA (3.5 mm)
12 × SA	12 × proximal	10 × AS	6 × balloon-expandable stent (7–8 mm)
		1 × RAD	1 × self-expandable stent (10 mm)
		1 × RES	5 × PTA (8 mm)

Note.—ICA = internal carotid artery; ECA = external carotid artery; CCA = common carotid artery; IA = innominate artery; VA = vertebral artery; SA = subclavian artery; AS = atherosclerosis; FMD = fibromuscular dysplasia; RES = restenosis; RAD = radiation therapy.

diffusion abnormalities after angioplasty or angioplasty plus stenting of arteries supplying the brain, other than at the carotid bifurcation. Therefore, we prospectively obtained diffusion-weighted MR images of the brain before and after such revascularization procedures.

Methods

Patients

This prospective study comprises interventional revascularization procedures of arteries supplying the brain, other than at the carotid bifurcation, performed during 12 months at our institution. During that period, a total of 47 such revascularization procedures were performed in 40 patients (Table 1). The inclusion criterion was the ability to perform MR imaging of these patients. Therefore, this series is a nonconsecutive one. Thirty-seven interventions were performed in 32 patients who were eligible to be enrolled in the study. In five patients, two procedures were performed with a time difference between the procedures of between 6 weeks and 6 months.

The average age of the patients was 62 years (range, 39–80 years). Nineteen male and 13 female patients were treated. All patients had symptoms related to the vascular territory to be treated during the last 6 months before the intervention. Eleven procedures were performed at the distal internal carotid artery (ICA), two at the external carotid artery, two at the common carotid artery, five at the innominate artery, five at the vertebral artery (VA), and 12 at the subclavian artery (SA). Six of the 37 procedures were performed on intradural, intracranial lesions. The lesions of the SA were all situated proximal to the origin of the VA. In all 12 lesions of the SA, the patients had subclavian steal phenomena of the affected side. In the q5 lesions of the innominate artery, right subclavian steal phenomena were present. In only one of these five cases, carotid steal phenomena were also shown. In both patients with lesions of the external carotid artery, there was a concomitant occlusion of the ICA of the ipsilateral side and branches of the external carotid artery were supplying the ipsilateral carotid siphon and the middle cerebral artery. Of the 37 lesions, there were 35 stenoses, with an average stenosis grade of 79% (range, 57–90%), measured according to the North American Symptomatic Carotid Endarterectomy Trial method (27), and two occlusions of the SA. Each patient underwent a neurologic examination before and 24 hours after the procedure.

Procedure

The day before the procedure, the patients received 500 mg of acetylsalicylic acid and 300 mg of clopidrogel. The daily administration of 100 mg of acetylsalicylic acid was continued as permanent medication, and the daily administration of an additional 75 mg of clopidrogel was continued for 3 months. All procedures were performed with the patient under local anesthesia, with percutaneous transfemoral access; in three cases, an additional transbrachial approach was used (Table 1). During the procedure, the patients received 5000 to 10,000 IU of heparin, administered intraarterially, to achieve an activated clotting time of more than 200 seconds. In each case, the procedure started with four-vessel cerebral angiography. Thereafter, a 7- to 8-F 80- to 100-cm-long sheath was used for lesions of the innominate artery, common carotid artery, and SA and a 5- to 6-F 100-cm-long guiding catheter was used for lesions of the ICA, external carotid artery, and VA. By using the sheath and/or guiding catheter in road map or overlay technique, the lesion was visualized. After crossing the lesion with a guidewire, in all cases, balloon angioplasty with appropriate balloon size was performed. For intracranial lesions, the balloon was deliberately undersized. If angiographic control after balloon angioplasty showed an unsatisfactory result, stent implantation was performed. The self-expandable stents were post-dilated. Finally, angiography of the percutaneous transluminal angioplasty and/or stent site and intracranial circulation of the treated vessel was performed. One hour after the procedure, with an activated clotting time of less than 140 seconds and a neurologically and hemodynamically stable patient condition, the arterial sheath was removed with a vascular occlusion device.

Imaging Technique

MR imaging was performed on a 1.5-T MR whole-body MR system with a head coil. The MR studies consisted of axial T2- and diffusion-weighted sequences. The T2-weighted sequence was a fast spin-echo sequence (single echo; 5700/119 [TR/TE]; echo train length, 15; matrix, 240 × 512; field of

view, 201 × 230 mm; number of excitations, one; section thickness, 5 mm; intersection gap, 1.5 mm; total acquisition time, 1.36 min). The diffusion-weighted sequence was a spin-echo/echo-planar sequence (6000/103; matrix, 96 × 200; field of view, 230 × 230 mm; section thickness, 5 mm; intersection gap, 1.5 mm; number of excitations, one; fat saturation; total acquisition time, 0.30 min). The MR diffusion sequence was run at two levels of diffusion sensitization (b = 0 and b = 1000 s/mm^2). The higher level of diffusion sensitization was replicated in each of the three principal gradient directions (x, y, and z planes). The diffusion-weighted MR images were displayed as diffusion-weighted images in the three directions.

MR imaging was performed before and 24 hours after the procedures. On the T2-weighted images, the presence of previous territorial infarction was determined. On the diffusion-weighted MR images, the presence of a signal abnormality was recorded. For all diffusion-weighted abnormalities, the size, vascular distribution, lobe, and area of brain in which the lesion occurred were determined. The upper area was defined as the cerebral area above the lateral ventricles, middle as the area between the lateral and third ventricles, and lower as the cerebral area below the third ventricle. For the anterior circulation, ipsilateral was defined as the side that was treated and contralateral as the side that was not treated. All diffusion-weighted abnormalities were correlated with the findings of the T2-weighted images. The results of the pre- and postprocedural MR imaging were compared, and new lesions were defined as lesions that were present only on the postprocedural MR images. All MR examinations were evaluated by two neuroradiologists who were unaware of the procedure performed. In case of dissent, the examinations were reviewed by a third neuroradiologist and a decision was made by consent.

Results

Procedures

Thirty-four (92%) of the 37 procedures were successfully completed, including the two cases of SA occlusion. Three stenoses of the cavernous part of the ICA could be crossed with a guidewire but not with the angioplasty balloon. In the 34 completed procedures, the grade of stenosis after intervention was reduced to an average of 12% (range, 0–50%). In 16 (47%) of 34 completed procedures, a stent was implanted to improve the angioplasty result. The control angiography of the intracranial circulation after completion of the procedure did not show any evidence for distal embolization. The neurologic examinations performed 24 hours after the procedure showed that none of the patients had new neurologic symptoms or deficits (Table 1 and Figs 1–4).

MR Imaging

Previous territorial infarction could be seen on the T2-weighted images obtained before the procedure for 14 (44%) of 32 patients. Eight of the 14 infarctions had occurred in the vascular territory to be treated. None of the infarction occurred in the posterior circulation of patients with lesions of the innominate artery or SA (Table 2 and Figs 1–3).

A total of five hyperintense lesions were shown on three of the 37 preprocedural diffusion-weighted MR images. One patient with a left proximal SA stenosis had one hyperintense lesion revealed (5–10 mm, left middle cerebral artery territory, parietal lobe); one patient with a stenosis of the origin of the left VA had one hyperintense lesion revealed (20 mm, right posterior cerebral artery [PCA] territory, occipital lobe); one patient with a stenosis of the V4 segment of the left VA had three hyperintense lesions revealed (5–10 mm, left PCA territory, occipital lobe). The last patient also had a new postprocedural lesion revealed on the diffusion-weighted images (Table 2, patient 8).

On eight (22%) of the 37 postprocedural diffusion-weighted MR images, a total of 35 new hyperintensities were visible (Figs 1–3). All these lesions were focal in nature. An average of 4.4 (range, 1–17) lesions occurred. Twenty-seven lesions were found in the middle cerebral artery territory, two in the PCA territory, four in the superior cerebellar artery territory, and two in the posterior inferior cerebellar artery territory. Twenty-eight of the 29 lesions in the vascular territory of the middle cerebral artery and PCA were found in the cortical area. Twenty-two lesions were seen in the parietal lobe, three in the frontal lobe, two in the temporal lobe, one in the occipital lobe, one in the thalamus, and six in the cerebellum. None of the lesions occurred in the brain stem. Twenty-four lesions had diameters < 5 mm, eight had diameters between 5 and 10 mm, one had a diameter of 15 mm, and two had diameters of 20 mm. Of the 29 lesions of the cerebrum, 16 occurred in the upper area, seven in the middle area, and six in the lower area.

In association with six of the eight procedures for which new postprocedural lesions were revealed by diffusion-weighted MR imaging, the lesions occurred in the vascular territory supplied by the treated vessel. In a patient in whom percutaneous angioplasty of the origin of the external carotid artery was performed, one lesion occurred in the cerebellum (Table 2, patient 4). In a patient in whom percutaneous angioplasty of a stenosis of the cervical ICA without cross flow to the contralateral side was performed, one lesion occurred in the contralateral hemisphere (Table 2, patient 3). Therefore, 33 (94%) of the 35 lesions occurred in the vascular territory supplied by the treated vessel. None of the lesions occurred after procedures at the SA in the vascular territory supplied by this vessel. Excluding the procedures of the SA, in association with six (24%) of 25 procedures, new hyperintense lesions in the vascular territory supplied by the treated vessel were visible on the diffusion-weighted MR images. In one case (Table 2, patient 1, and Fig 1), new lesions were detected after guidewire and/or catheter manipulation without performing angioplasty. In one patient (Table 2, patient 2), ipsi- and contralateral lesions occurred after percutaneous angioplasty of the cavernous part of the ICA, with a contralateral occlusion of the ICA. In one patient (Table 2, patient 5, and Fig 2), lesions occurred in the PCA territory after stent implantation of the origin of the innominate artery. In this pa-

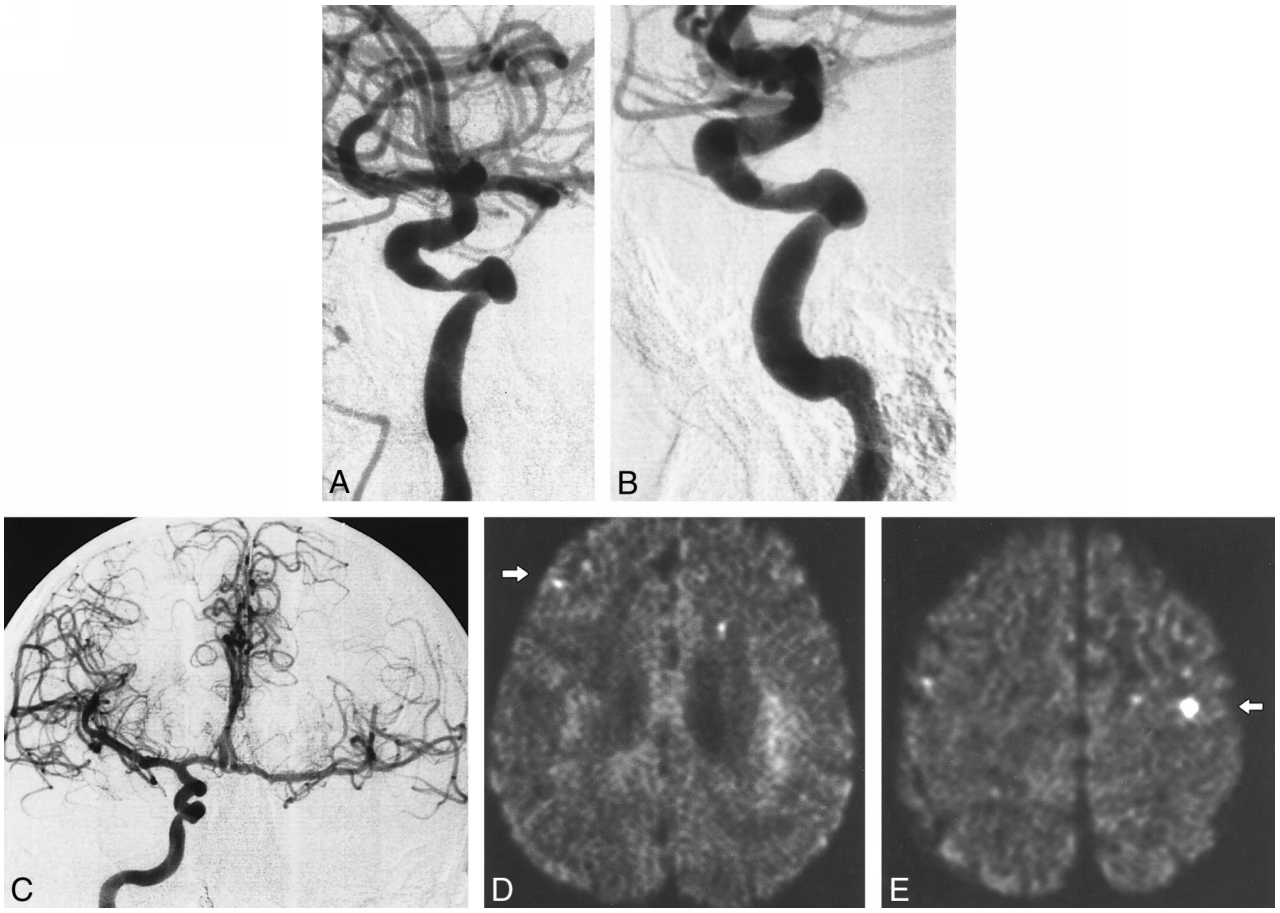

FIG 1. Patient 2.
A, Stenosis of the cavernous part of the right ICA.
B, Result after percutaneous angioplasty (3.5-mm balloon). Note irregularity at the site of the percutaneous angioplasty.
C, Cross flow from the right ICA to the contralateral hemisphere (occlusion of the left ICA is not shown). Post-procedural diffusion-weighted images (6000/103; number of excitations, one) obtained with a diffusion sensitization level of b = 1000 s/mm^2.
D, New ipsilateral lesion: <5 mm, middle cerebral artery cortical territory, parietal lobe (*arrow*).
E, New contralateral lesion: 5 to 10 mm, middle cerebral artery cortical territory, parietal lobe (*arrow*).

tient, there was a congenital origin of both PCA from the respective ICA.

Ten (29%) of the 35 hyperintense lesions shown on the diffusion-weighted MR images were also visible on the T2-weighted images. Three (13%) of 24 lesions that were < 5 mm, four (50%) of eight lesions that were between 5 and 10 mm, one (100%) of one lesion that was 15 mm, and two (100%) of two of lesions that were 20 mm were visible on the T2-weighted images.

Discussion

Jordan et al (16) determined the rate of emboli detected by transcranial Doppler monitoring during stent implantation of the carotid bifurcation, with a mean of 74.0 emboli per procedure. During only three (7.5%) procedures were no emboli detected. The authors showed that the majority of the emboli were connected to the guidewire and/or catheter manipulation and the deflation of the balloon. However, they could not find a direct relationship between the number of emboli and the neurologic events of the patients. Ohki et al (14) showed, in an ex vivo model of the carotid bifurcation, that distal embolization was observed in all cases during stent implantation of the carotid bifurcation. They observed a median of 15 emboli, with range of two to 126 per procedure. Manninen et al (15) showed that in cadavers in situ during stent implantation of the carotid bifurcation, distal embolization occurred in all cases during stent placement and post dilation. It can be assumed that similar rates of emboli can occur with revascularization procedures of arteries supplying the brain other than at the carotid bifurcation.

Diffusion-weighted MR imaging of the brain is the diagnostic procedure with the highest sensitivity for ischemic cerebral events (17–23). Burdette et al (19) showed that in all cases, 24 hours after cerebral infarction, abnormal signal intensity was evident on diffusion-weighted MR images. Because neurologic events after revascularization procedures of vessels supplying the brain are rare and because transcranial Doppler monitoring has shown that many emboli are asymptomatic, we used dif-

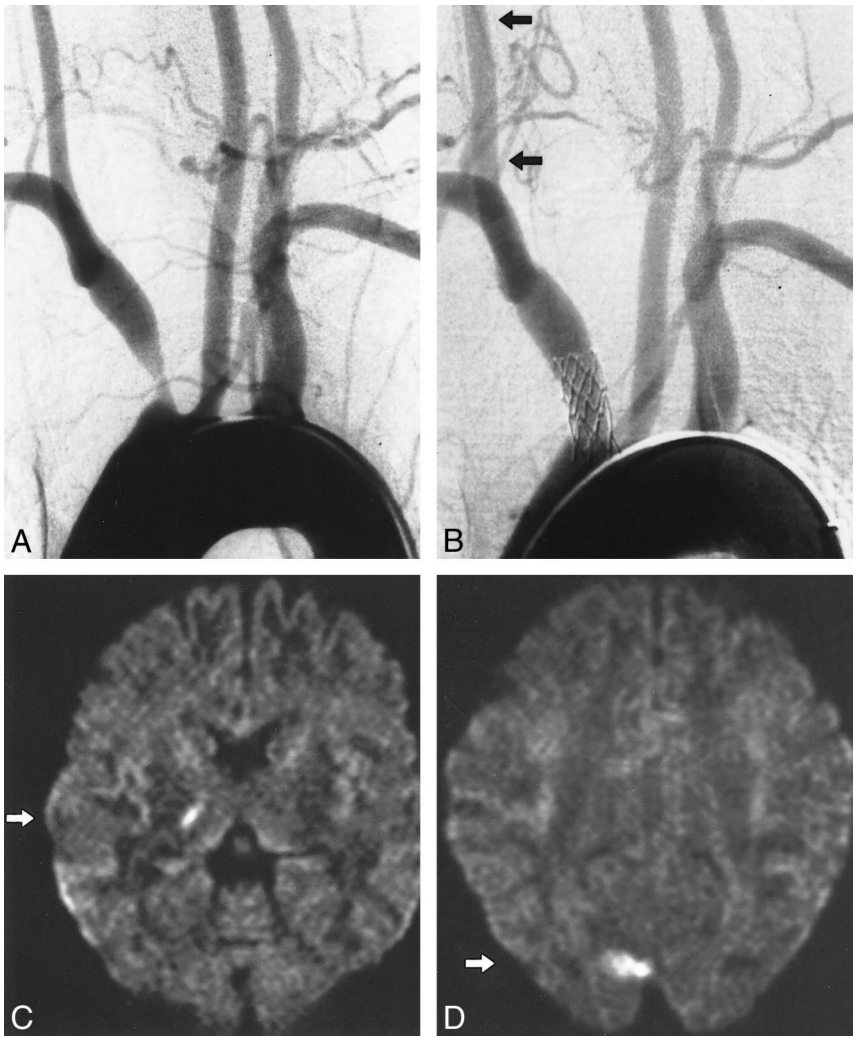

FIG 2. Patient 5.

A, Aortic arch injection (early phase). Stenosis of the innominate artery with antegrade flow in the right carotid artery. (Retrograde flow in the right VA with subclavian steal in the late phase is not shown).

B, Result after stent implantation (balloon-expandable stent, 8 mm diameter) with antegrade flow in the right VA (*arrows*). Post-procedural diffusion-weighted images (6000/103; number of excitations, one) obtained with a diffusion sensitization level of b = 1000 s/mm^2.

C, New ipsilateral lesion: 5 to 10 mm, PCA deep territory, thalamus (*arrow*).

D, New ipsilateral lesion: 15 mm, PCA cortical territory, occipital lobe (*arrow*).

fusion-weighted MR imaging before and 24 hours after the procedure to determine the incidence of new lesions after such interventions.

In eight (22%) of the 37 postprocedural diffusion-weighted MR images, a total of 35 new hyperintense lesions occurred; 33 (94%) of the 35 lesions occurred in the vascular territory supplied by the treated vessel. This indicates that the cause of these signal abnormalities is emboli released during the procedure and delivered into the distal circulation of the treated vessel.

In association with procedures of vessels that supply the anterior circulation (ICA, external carotid artery, and innominate artery), the majority of lesions occurred in the distribution of the cortical branches of the middle cerebral artery, the parietal lobe, and the upper area of the brain, with a diameter < 5 mm. This type and distribution of lesions can be considered as the ''embolic pattern'' of cerebral embolization. This pattern can be explained in that emboli released during the procedure will take the straight way up into cortical branches of the middle cerebral artery and get stuck in small and medium arteries at the top of the brain.

In one case in our series, lesions occurred in the distribution of the ipsi- and contralateral middle cerebral artery after percutaneous angioplasty of the ICA, with occlusion of the contralateral ICA. In these circumstances, embolization through the anterior communicating artery to the contralateral side has to be assumed. In another case, lesions occurred in the distribution of the PCA after stent implantation of the innominate artery, with congenital origin of both PCA from the respective ICA. In this patient, subclavian steal phenomena of the right VA occurred before the procedure, protecting the posterior circulation from embolization through the VA. In these circumstances, embolization through the posterior communicating artery to the PCA has to be assumed. These two cases illustrate that embolization through the anterior communicating artery and posterior communicating artery is possible and that the flow will determine where the emboli will occur. For every case, the ''brain at risk'' of embolization has to be determined after preprocedural angiography of the complete cerebral circulation, taking these findings into consideration.

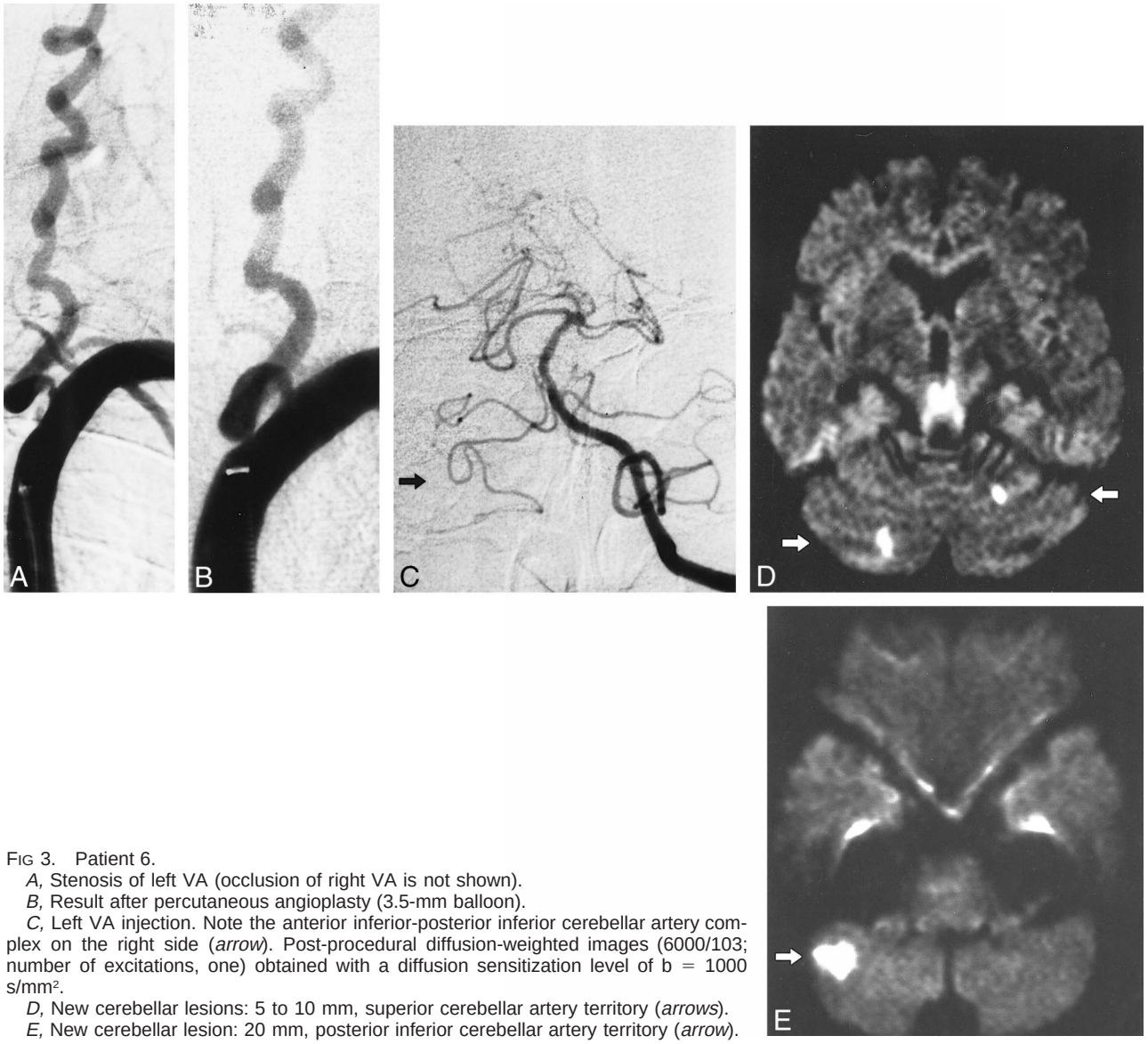

FIG 3. Patient 6.
A, Stenosis of left VA (occlusion of right VA is not shown).
B, Result after percutaneous angioplasty (3.5-mm balloon).
C, Left VA injection. Note the anterior inferior-posterior inferior cerebellar artery complex on the right side (*arrow*). Post-procedural diffusion-weighted images (6000/103; number of excitations, one) obtained with a diffusion sensitization level of b = 1000 s/mm^2.
D, New cerebellar lesions: 5 to 10 mm, superior cerebellar artery territory (*arrows*).
E, New cerebellar lesion: 20 mm, posterior inferior cerebellar artery territory (*arrow*).

In association with procedures of the VA, all lesions occurred in the cerebellum in the distribution of the superior cerebellar and posterior inferior cerebellar arteries. A likely explanation of this distribution is that the perforating branches of the basilar and anterior inferior cerebellar arteries have as small a size and as rectangular an origin as the basilar artery; therefore, flow will direct emboli into the superior cerebellar artery territory and posterior inferior cerebellar artery territory. This pattern of embolization could also account for the low incidence of embolic complications reported in the literature for revascularization procedures of the vertebrobasilar arteries, despite the important brain areas supplied by these vessels (9, 11–13).

None of the postprocedural lesions in the diffusion-weighted MR images occurred after procedures of the SA. All patients with stenoses and/or occlusions of the SA had subclavian steal phenomena of the affected side. Ringelstein and Zeumer (8) showed that after sufficient revascularization of the proximal SA, the flow direction within the VA did not immediately change to antegrade but did so gradually, within 20 seconds up to several minutes. This delay of flow reversal is thought to serve as a protective mechanism against cerebral embolism during and shortly after revascularization of the proximal SA. This is in agreement with the very low incidence of cerebral events with angioplasty for subclavian steal phenomena reported by others (5, 6). This supports angioplasty and stenting of the SA as a low risk alternative to surgical revascularization of proximal disease of the SA.

Of note is that we found, in two patients, lesions in a territory of the brain not supplied by the treated vessel. One lesion was found in the contralateral hemisphere after percutaneous angioplasty of the ICA without cross flow from the treated side and one was found in the cerebellum after percutaneous angioplasty of the origin of the external carotid ar-

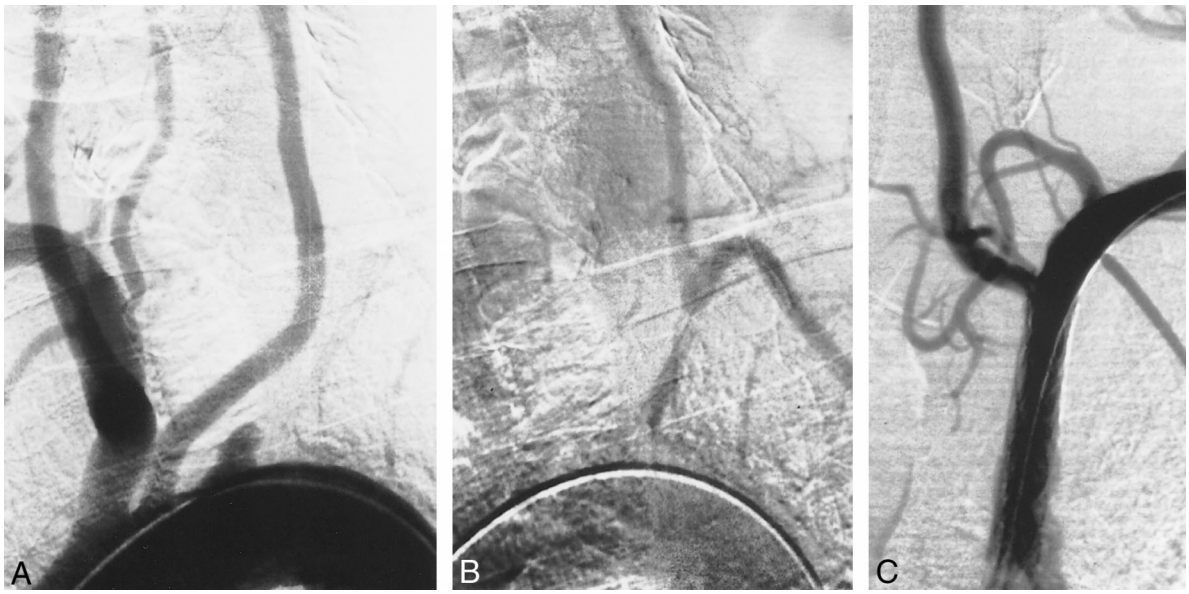

FIG 4. *A,* Aortic arch injection (early phase). Occlusion of the proximal part of the left SA.
B, Aortic arch injection (late phase). Retrograde flow in left VA with subclavian steal.
C, Result after stent implantation (balloon-expandable stent, 7 mm) with antegrade flow in left VA.

TABLE 2: Characteristics of new postprocedural lesion in DW-MR imaging

Patient No.	Treated Vessel	Lesions (N)	Side of Lesion	Vascular Distribution	Lobe	Area	Size (mm)	Comments
1	ICA, cavernous	7	Ipsilateral	7 × MCA	7 × parietal	2 × upper 5 × middle	6 × <5 1 × 5–10	Attempt to treat; not possible to cross lesion with guidewire
2	ICA, cavernous	6 11	Ipsilateral Contralateral	6 × MCA cortical 11 × MCA cortical	6 × parietal 3 × frontal 8 × parietal	6 × upper 6 × upper 5 × lower	6 × <5 10 × <5 1 × 5–10	3.5-mm PTA: cross-flow to contralateral side; occlusion of contralateral ICA
3	ICA, cervical	1	Contralateral	1 × MCA cortical	1 × parietal	1 × upper	1 × 20	PTA (5 mm); FMD; no cross-flow to contralateral side
4	ECA, origin	1	—	1 × SCA	1 × cerebellar	—	1 × <5	PTA (4 mm)
5	IA origin	4	Ipsilateral	2 × MCA cortical 1 × PCA cortical 1 × PCA deep	2 × temporal 1 × occipital 1 × thalamic	1 × upper 2 × middle 1 × lower	1 × <5 2 × 5–10 1 × 15	Balloon-expandable stent (8 mm); subclavian steal right, no carotid steal
6	VA V1	3	—	2 × SCA 1 × PICA	3 × cerebellar	—	2 × 5–10 1 × 20	PTA (3.5 mm); occlusion of contralateral VA
7	VA V1	1	—	1 × PICA	1 × cerebellar	—	1 × 5–10	Balloon-expandable stent (3.5 mm); occlusion of contralateral VA
8	VA V4	1	—	1 × SCA	1 × cerebellar	—	1 × 5–10	Balloon-expandable stent (3.5 mm); occlusion of contralateral VA

Note.—ICA = internal carotid artery; IA = innominate artery; VA = vertebral artery; MCA = middle cerebral artery; PCA = posterior cerebral artery; AICA = anterior inferior cerebellar artery; PICA = posterior inferior cerebellar artery; SCA = superior cerebellar artery; FMD = fibromuscular dysplasia.

tery without collateralization to the posterior circulation. Bendszus et al (24) found, in 26% of all patients after diagnostic cerebral angiography, new lesions on the diffusion-weighted MR images of the brain. All our patients had undergone complete cerebral angiography before undergoing the procedure. This indicates that the guidewire and/or catheter manipulation of a diagnostic study alone can cause lesions in the diffusion-weighted MR images.

Van Everdingen et al (22) reported that diffusion-weighted MR imaging detected 98% of all ischemic lesions, in contrast to fluid-attenuated inversion recovery, proton density-weighted, and T2-weighted sequences that showed only 91%, 80%, and 71% of all lesions, respectively. In our

series, only 10 (29%) of the 35 lesions were visible in the T2-weighted sequence. The smaller the lesions were, the less likely they were to be seen on the T2-weighted images. This emphasizes that results of diffusion-weighted MR imaging regarding the number of cerebral lesions cannot be compared with other MR imaging studies and that diffusion-weighted MR imaging should be considered as the standard of reference for the detection of cerebral lesions after interventional procedures of vessels supplying the brain.

It is not yet completely understood which histologic basis the signal changes on diffusion-weighted MR images represent. Kidwell et al (21) showed that 20% of patients with transient ischemic attack who had early diffusion-weighted abnormalities did not have evidence of established infarction shown by follow-up MR imaging. On the other hand, once a cell shows a signal increase on the diffusion-weighted MR images, the time frame in humans for restoration of oxygen and metabolite supply and reversibility may be very narrow (20). Therefore, a signal abnormality on diffusion-weighted MR images obtained 24 hours after the occurrence should be considered as an early marker of infarction. Follow-up MR imaging studies of patients with signal abnormalities on diffusion-weighted MR images after interventional procedures of vessels supplying the brain will shed more light on this topic.

At present, it is not known which step of the procedure may be responsible for the majority of these lesions. In one of our patients, ipsilateral lesions occurred after crossing the lesion with a guidewire without actually performing the balloon angioplasty. Emboli could occur during diagnostic angiography and the introduction of the long sheath and/or guiding catheter. They may also occur during the initial crossing of the stenosis with the guidewire or during balloon angioplasty, stent placement, and/or post-dilation of the stent (14–16). Further investigations with transcranial Doppler monitoring during the procedures are necessary to clarify this matter.

There is some controversy regarding the clinical importance of cerebral microemboli. Ohki et al (14) reported that the average size of particles was 338 μ (range, 120–2100 μ) during stent implantation of the carotid bifurcation. In our series, no permanent neurologic symptom or deficit occurred. On the other hand, there may be important intracerebral arteries as small as 100 μ in diameter. Lövblad et al (26) reported that new ipsilateral lesions were revealed by the diffusion-weighted MR images of four of 19 patients after stent implantation of the carotid bifurcation; two of the four patients were neurologically symptomatic. It has not yet been determined whether the number and/or size of cerebral emboli is related to the occurrence of neurologic events. The relationship between iatrogenic emboli and neurologic effect remains to be more precisely defined.

Despite this uncertainty, it has to be assumed that fewer emboli, and consequently fewer lesions, on diffusion-weighted MR images may be beneficial to the patient. Devices for cerebral protection during stent implantation at the carotid bifurcation have been used, such as occlusion balloons and filters (28, 29). In the future, the development of such protection devices should be extended to protect also interventions at the origin of supraaortal arteries and at more distal intracranial vessels.

Conclusion

Revascularization procedures of arteries supplying the brain were associated with new lesions revealed by diffusion-weighted MR imaging of the brain after 22% of the procedures, provided that MR imaging could be performed, indicating the occurrence of cerebral microemboli during such procedures. Diffusion-weighted MR imaging of the brain can be used as a tool to assess the impact of modifications of procedural technique and/or the use of cerebral protection devices on the occurrence of such lesions.

Acknowledgments

The authors thank Walter Kuehn for preparation of the photographic work.

References

1. Wholey MH, Wholey M, Mathias K, et al. **Global experience in cervical carotid artery stent placement.** *Catheter Cardiovasc Interv* 2000;50:160–167
2. Wholey MH, Wholey MH, Jannolowski CR, Eles G, Levy D, Buechtel J. **Endovascular stents for carotid artery occlusive disease.** *J Endovasc Surg* 1997;4:326–338
3. Yadav JS, Roubin GS, Iyer S, et al. **Elective stenting of the extracranial carotid arteries.** *Circulation* 1997;95:376–381
4. Diethrich EB, Ndiaye M, Reid DB. **Stenting in the carotid artery: initial experience in 110 patients.** *J Endovasc Surg* 1996; 3:42–62
5. Kumar K, Dorros G, Bates MC, Palmer L, Mathiak L, Dufek C. **Primary stent deployment in occlusive subclavian artery disease.** *Cathet Cardiovasc Diagn* 1995;34:281–285
6. Mathias KD, Luth I, Haarmann P. **Percutaneous transluminal angioplasty of proximal subclavian artery occlusions.** *Cardiovasc Intervent Radiol* 1993;16:214–218
7. Vitek JJ. **Subclavian artery angioplasty and the origin of the vertebral artery.** *Radiology* 1989;170:407–409
8. Ringelstein EB, Zeumer H. **Delayed reversal of vertebral artery blood flow following percutaneous transluminal angioplasty for subclavian steal syndrome.** *Neuroradiology* 1984;26: 189–198
9. Chastain HD, Campbell MS, Iyer S. **Extracranial vertebral artery stent placement: in-hospital and follow-up results.** *J Neurosurg* 1999;91:547–552
10. Eckard DA, Zarmov DM, McPherson CM, et al. **Intracranial internal carotid artery angioplasty: technique with clinical and radiographic results and follow-up.** *AJR Am J Roentgenol* 1999; 172:703–707
11. Higashida RT, Tsai FY, Halbach VV, et al. **Transluminal angioplasty for atherosclerotic disease of the vertebral and basilar arteries.** *J Neurosurg* 1993;78:192–198
12. Horowitz MB, Pride GL, Graybeal DF, et al. **Percutaneous transluminal angioplasty and stenting of midbasilar stenoses: three technical case reports and literature review.** *Neurosurgery* 1999;45:925–930
13. Connors JJ, Wojak JC. **Percutaneous transluminal angioplasty for intracranial atherosclerotic lesions: evolution of technique and short-term results.** *J Neurosurg* 1999;91:415–423

14. Ohki T, Marin ML, Lyon RT. **Ex vivo human carotid artery bifurcation stenting: correlation of lesion characteristics with embolic potential.** *J Vasc Surg* 1998;27:463–471
15. Manninen HI, Rasanen HT, Vanninen RL, Vainio P, Hippelainen M, Kosma VM. **Stent placement versus percutaneous transluminal angioplasty of human carotid arteries in cadavers in situ: distal embolization and findings at intravascular US, MR imaging and histopathologic analysis.** *Radiology* 1999;212: 483–492
16. Jordan WD, Voellinger DC, Doblar DD, Plyushcheva NP, Fisher WS, McDowell HA. **Microemboli detected by transcranial Doppler monitoring in patients during carotid angioplasty versus carotid endarterectomy.** *Cardiovasc Surg* 1999;7:33–38
17. Beauchamp NJ, Barker PB, Wang PY, van Zijl PC. **Imaging of acute cerebral ischemia.** *Radiology* 1999;212:307–324
18. Burdette JH, Elster AD, Ricci PE. **Acute cerebral infarction: quantification of spin density and T2 shine-through phenomena on diffusion-weighted MR images.** *Radiology* 1999;212: 333–339
19. Burdette JH, Ricci PE, Petitti N, Elster AD. **Cerebral infarction: time course of signal intensity changes on diffusion-weighted MR images.** *AJR Am J Roentgenol* 1998;171:791–795
20. Beauchamp NJ, Ulug AM, Passe TJ, van Zijl PC. **MR diffusion imaging in stroke: review and controversies.** *Radiographics* 1998;18:1269–1285
21. Kidwell CS, Alger JR, Di Salle F, et al. **Diffusion MRI in patients with transient ischemic attacks.** *Stroke* 1999;30:1174–1180
22. Van Everdingen KJ, van der Grond J, Kapelle LJ, Ranios LM, Mali WP. **Diffusion-weighted magnetic resonance imaging in acute stroke.** *Stroke* 1998;29:1783–1790
23. Lövblad K, Laubach H, Baird AE, et al. **Clinical experience with diffusion-weighted MR in patients with acute stroke.** *AJNR Am J Neuroradiol* 1998;19:1061–1066
24. Bendszus M, Koltzenburg M, Burger R, Warmuth-Metz M, Hofmann E, Solymosi L. **Silent embolism in diagnostic cerebral angiography and neurointerventional procedures: a prospective study.** *Lancet* 1999;354:1594–1597
25. Britt PM, Heiserman JE, Robb M, et al. **Incidence of postangiographic abnormalities revealed by diffusion-weighted MR imaging.** *AJNR m J Neuroradiol* 2000;21:55–59
26. Lövblad KO, Phischke W, Remonda L, et al. **Diffusion-weighted MRI for monitoring neurovascular interventions.** *Neuroradiology* 2000;42:134–138
27. Fox AJ. **How to measure carotid stenosis.** *Radiology* 1993;186: 316–318
28. Theron JG, Payelle GG, Coskun O, et al. **Carotid artery stenosis: treatment with protected balloon angioplasty and stent placement.** *Radiology* 1996;201:627–636
29. Ohki T, Roubin GS, Veith FJ, Iyer SS, Brady E. **Efficacy of a filter device in the prevention of embolic events during carotid angioplasty and stenting: an ex vivo analysis.** *J Vasc Surg* 1999; 30:1034–1044